Mn-rich clusters in GeMn magnetic semiconductors: Structural evolution and magnetic property

Yong Wang [a,*], Faxian Xiu [b], Ya Wang [a], Xufeng Kou [b], Ajey P. Jacob [c], Kang L. Wang [b], Jin Zou [a,d]

[a] Materials Engineering, The University of Queensland, Brisbane, QLD 4072, Australia
[b] Electrical Engineering Department, University of California at Los Angeles, CA 90095, USA
[c] Intel assignee to Western Institute of Nanoelectronics (WIN) Intel Corporation, 2200 Mission College Blvd, Santa Clara, CA 95052, USA
[d] Centre for Microscopy and Microanalysis, The University of Queensland, Brisbane, QLD 4072, Australia

ABSTRACT

The structural evolution and magnetic property of Mn-rich clusters in GeMn thin films grown at 70 °C by molecular beam epitaxy has been systematically investigated by TEM, EDS and SQUID. It was discovered that, by controlling the Mn concentration, the morphology of coherent Mn-rich clusters can be manipulated from tadpole to nanocolumn shapes. For a particular Mn concentration, the critical thickness to form coherent Mn-rich clusters at 70 °C has been identified. Magnetic measurements show a complex magnetic behavior, which is mainly related to the Mn-rich clusters or precipitates. Our results also reveal that a flat surface of the Ge buffer layer plays an important role in producing vertically aligned tadpoles and nanocolumns.

© 2010 Elsevier B.V. All rights reserved.

1. Introduction

Diluted magnetic semiconductors (DMSs), possessing both magnetic and semiconducting properties, have been extensively investigated due to their promising applications in spintronic devices [1–4]. Being compatible with current Si technology, $Ge_xMn_{1−x}$ DMSs have attracted particular attention and extensive studies have been carried out to investigate their nanostructures and magnetic properties, both experimentally and theoretically [5–14]. It is well understood that inhomogeneous Mn doping in Ge thin films tends to generate Mn-rich magnetic intermetallic precipitates (such as Mn_5Ge_3 [15–20] and $Mn_{11}Ge_8$ [21–23]), or coherent Mn-rich clusters (such as tadpoles [24] and nanocolumns [13,25,26]), due to the low solubility of Mn in Ge. Basically, low growth temperature and low Mn concentration are favorable for the formation of coherent Mn-rich clusters, otherwise, secondary intermetallic precipitates will be developed. For example, Bougeard et al. [27] reported coherent Mn-rich clusters in precipitate-free $Ge_{0.95}Mn_{0.05}$ films on Ge substrates grown at 60 °C. Increasing the growth temperature to 70 °C, they revealed the co-existence of secondary Mn_5Ge_3 precipitates and coherent Mn-rich clusters [16], which is similar to our previous study where coherent Mn-rich clusters dominate the film with Mn_5Ge_3 precipitates occasionally seen in the $Ge_{0.96}Mn_{0.04}$ thin films on Si grown at 70 °C [24]. When the growth temperature is risen to 120 °C or above, secondary precipitates, such as Mn_5Ge_3 and $Mn_{11}Ge_8$, dominate the grown thin films, as well documented in the literature [15–19,21–23]. Nevertheless, these studies were mainly focused on individual type of Mn-rich clusters or precipitates; and little attention has been paid to comprehensively understand the dynamic growth (structural evolution) of these Mn-rich clusters. More importantly, the mechanism of Mn diffusion and the formation of different morphologies of Mn-rich clusters (such as nanocolumns) remain unclear and deserve an urgent investigation in order for this type of DMS thin films to be practically applicable.

In this letter, through detailed transmission electron microscopy (TEM) and energy dispersive X-ray spectroscopy (EDS) investigations, we demonstrate the structural evolution of coherent Mn-rich clusters driven by Mn diffusion. From which, the nature of Mn diffusion as well as the effect of the Ge buffer layer is clarified. In addition, the magnetic properties of the Mn-rich clusters are also discussed.

* Corresponding author.
E-mail addresses: y.wang4@uq.edu.au (Y. Wang), j.zou@uq.edu.au (J. Zou).

2. Experimental details

The $Ge_{1-x}Mn_x$ thin films with different nominal Mn concentrations (namely, $x = 0.025, 0.04, 0.045, 0.055, 0.070$ and 0.120, respectively) were grown on Ge (1 0 0) substrates at 70 °C using a Perkin-Elmer solid source MBE system. Prior to the growth, the Ge substrates were cleaned by the mixture of H_2SO_4:H_2O_2 (5:3) and diluted HF. The substrates were then annealed at 800 °C for 10 min in vacuum to remove the native oxide. A Ge buffer layer with a typical thickness of 35 nm was firstly deposited on a Ge (1 0 0) substrate at 400 °C, followed by the growth of Mn-doped Ge on the top of Ge buffer layer with a growth rate of 0.02 nm/s. For convenience, a shortened term is used to represent the samples hereafter. For example, S-2.5 denotes the $Ge_{1-x}Mn_x$ thin film with $x = 0.025$. The structural and chemical characteristics of grown thin films were characterized by TEM, high resolution TEM (HRTEM) and EDS. Cross-sectional TEM specimens were prepared by standard technique including mechanical polishing using a tripod technique and final ion-beam thinning using a Gatan precision ion polishing system. The TEM, HRTEM and EDS experiments were performed in a Philips Tecnai F20 TEM, operating at 200 kV.

3. Results and discussions

3.1. Structural evolutions

Fig. 1(a–f) presents typical cross-sectional TEM images of all grown $Ge_{1-x}Mn_x$ thin films, displaying their general morphology. Flat surfaces can be seen in all samples, which is different from the $Ge_{0.96}Mn_{0.04}$ thin films grown on Si where a rough surface was evi-

denced [24]. By carefully examining these images, vertically aligned tadpole-shaped clusters (dark contrast) can be observed [refer to Fig. 1(a–c)] with a tendency of the higher the Mn concentration, the higher the density of the tadpoles and the longer the tadpole tails. Indeed, the shape of these tadpoles is similar to those grown on Si substrates found in our previous study [24]. However, those tadpoles on Si are usually randomly orientated when compared with vertically aligned tadpoles found in this study (detailed discussion see later). With increasing the Mn concentration, the width of tadpole tails become thicker and tends to be identical to their heads, which eventually results in the formation of Mn-rich nanocolumns, as shown in Fig. 1(d). With further increasing the Mn concentration, the diameters of the nanocolumns increase, as displayed in Fig. 1(e and f). It has been shown that this kind of tadpoles possesses an identical structure of the diamond structured Ge matrix [13,24]. To identify the nature of our Mn-rich nanocolumns, extensive HRTEM investigations were conducted and a typical example is shown in Fig. 1(g). No lattice defects, such as dislocations, were observed and the Mn-rich nanocolumn has an identical structure with the Ge matrix, indicating a coherent nature between the nanocolumns and their surrounding Ge matrix, which agrees well with the previous results, where the formation of Mn-rich nanocolumns is induced by spinodal decomposition [13,25]. Quantitative EDS was employed
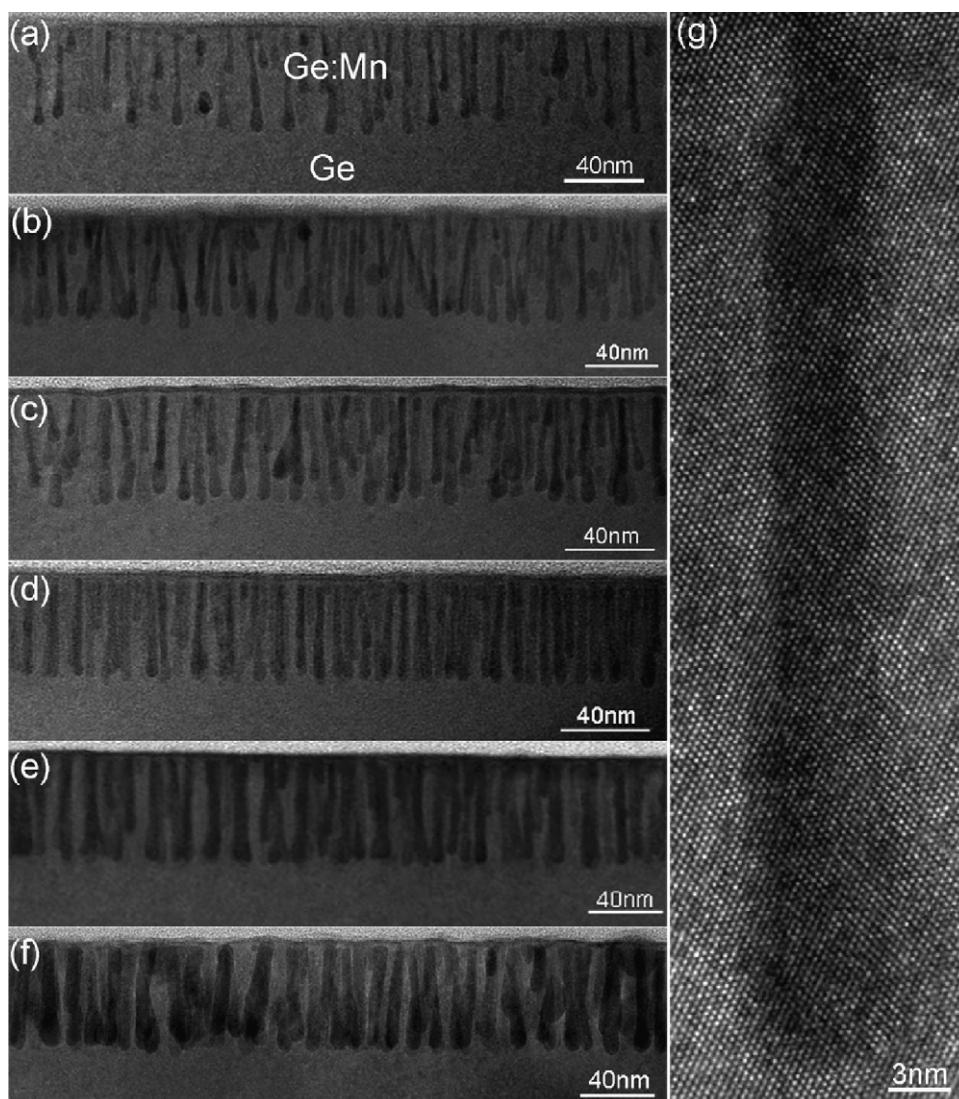

Fig. 1. Typical cross-sectional TEM images of samples: S-2.5 (a), S-4 (b), S-4.5 (c), S-5.5 (d), S-7 (e) and S-12 (f). (g) A typical HRTEM image of a coherent nanocolumn.
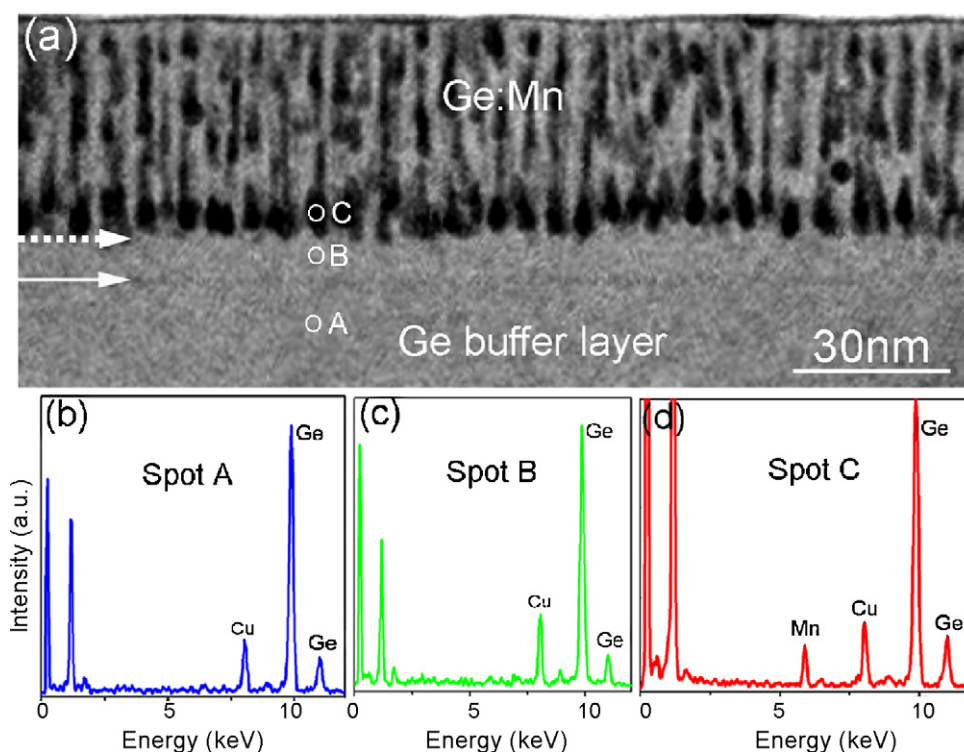
Fig. 2. (a) A TEM image of the Ge:Mn thin film with a distinguishable interfaces between the Ge buffer layer and the Ge:Mn thin film and where the tadpoles start; (b–d) typical EDS profile acquired from spots A, B and C in (a), respectively.

to measure the overall Mn concentration for these samples and the results show a good agreement with their respective nominal Mn concentrations. It should be noted that, although coherent Mn-rich tadpoles and nanocolumns dominate the thin films in these samples, Mn-rich precipitates, such as Mn_5Ge_3, can still be occasionally observed. Indeed, this result agrees with the results reported by Ahlers et al. [16], where a few Mn_5Ge_3 precipitates together with coherent clusters were observed in 5% Mn-doped Ge grown at 70 °C.

As can be seen from Fig. 1, Mn tends to diffuse to form coherent tadpoles and/or nanocolumns, other than homogenously distributed within the Ge matrix. However, to understand the Mn diffusion and subsequently the formation of these Mn-rich clusters, it is essential to distinguish the interface between the thin films and the Ge buffer layer. For this purpose, a dedicated $Ge_{1-x}Mn_x$ thin film (with nominal 3.5% Mn) with a distinguishable Ge buffer layer was prepared. Fig. 2(a) shows a typical TEM image of such a film, where two interfaces are distinguishable; i.e. the interface between the $Ge_{1-x}Mn_x$ thin films and the Ge buffer layer (marked by a white solid arrow) and the interface where the coherent Mn-rich clusters start (marked by a white dashed arrow). Obviously, a gap of ~12 nm between the two interfaces can be identified. To explore the composition variations across these interfaces, extensive EDS measurements in the scanning TEM mode were performed and typical results are shown in Fig. 2(b–d) for the spots A, B and C shown in Fig. 2(a). Interestingly, like the result in the Ge buffer layer (Fig. 2(b)), almost no Mn can be detected in the gap (spot B, Fig. 2(c)), which is similar to the results reported by Devillers et al., where they revealed that the Mn content in the Ge matrix is between 0% and 1% [13]. In strong contrast, quantitative EDS measurements show that up to 9% Mn can be found in the heads of tadpoles (e.g. spot C, Fig. 2(d)), which is significantly higher than the nominal composition of 3.5% Mn for this sample. This result indicates that, at the initial stage of the $Ge_{1-x}Mn_x$ thin film growth, Mn tends to diffuse towards to the surface, due to the misfit strain induced by larger Mn atoms (atomic radius: 140 pm) incorporation

into the Ge (atomic radius: 125 pm) lattice [11]. When the thickness of the $Ge_{1-x}Mn_x$ thin films reaches a critical value (~12 nm for this case) where, near the growth front, the local Mn concentration is sufficiently high and the spinodal decomposition takes place [13,24]. It should be noted that the critical thickness (the thickness threshold for the formation of Mn-rich clusters) varies with the nominal Mn concentration with a tendency of the higher the nominal Mn concentration, the smaller the critical thickness.

Based on the experimental results outlined above, a structural evolution of coherent Mn-rich clusters can be proposed, as schematically illustrated in Fig. 3(a). At the initial stage of the $Ge_{1-x}Mn_x$ thin film growth, Mn adatoms tend to remain in the growth front, causing an increased local Mn concentration. When the local Mn concentration is sufficient, the nucleuses of Mn-rich
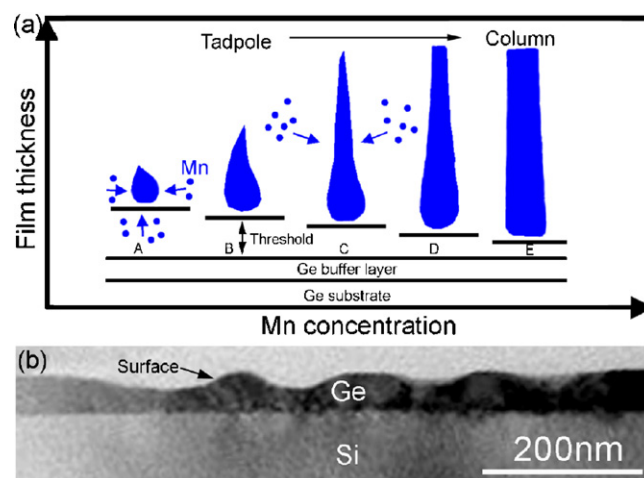

Fig. 3. (a) Schematic diagram of the structural evolution of Mn-rich clusters in the Ge:Mn thin films and (b) a TEM image of a Ge buffer layer grown on Si.
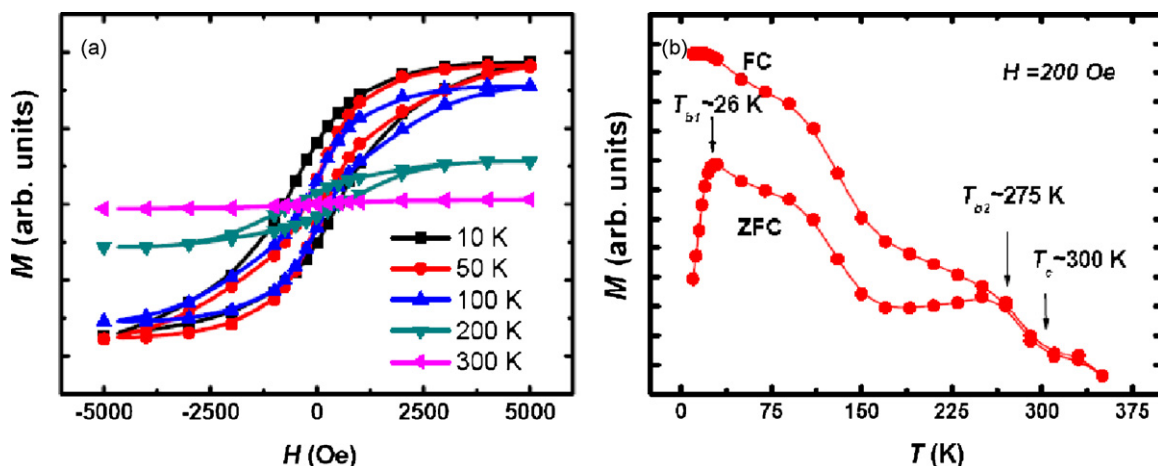
Fig. 4. SQUID measurements of a 5.5% Mn-doped Ge thin film grown on Ge substrate. (a) Hysteresis loops measured at different temperatures and (b) ZFC and FC curves measured with a magnetic field of 200 Oe.

clusters are formed, their physical locations are then locked (stage A) and subsequently they act as the nucleation sites for the cluster growth. With further growth of the $Ge_{1-x}Mn_x$ thin films, different consequences may be obtained depending upon the nominal Mn concentration: (1) if the nominal Mn concentration is low, tadpole-shaped Mn-rich clusters with a short tail will form as there is not enough Mn available in the growth front (stage B, also refer to Fig. 1(a)); (2) the tadpole tails become longer and larger when the nominal Mn concentration is slightly higher (stages C and D); (3) with higher nominal Mn concentration, coherent Mn-rich nanocolumns may be formed, as shown in stage E (also refer to Fig. 1(d)); and (4) when the nominal Mn concentration is very high, the size of the nanoclumns is increased (refer to Fig. 1(e and f)) and the Mn concentration within the coherent nanocolumns can reach up to 23%, confirmed by our extensive EDS measurements.

It is of interest to note that our tadpoles and nanocolumns are vertically aligned when compared with those randomly oriented tadpoles grown on Si substrates [24]. To understand this, we note flat interfaces between the $Ge_{1-x}Mn_x$ thin films and their underlying Ge buffer layer, as shown in Fig. 2(a), suggesting that the growth front of the Ge buffer layer is flat; which may be responsible to the vertically aligned tadpoles and nanocolumns. To clarify this point, we grew a comparative 35 nm Ge buffer layer on Si with the identical growth condition (e.g. the growth temperature of the Ge buffer layer being 400 °C). Fig. 3(b) is a typical TEM image of such a sample and shows a rough surface of the Ge buffer layer. As shown in Fig. 3(a), the surface of the Ge buffer layer is flat, which makes the tadpoles grow vertically and eventually form nanocolumns. This indicates that coherent Mn-rich clusters tend to grown along the normal direction of the growth front surface, which may explain the randomly oriented tadpoles in our previous results where a rough buffer layer surface was confirmed [24]. Taking all these results into account, we can conclude that flat buffer layer is vital to ensure a well aligned tadpoles and nanocolumns.

3.2. Magnetic properties

Superconducting quantum interference device (SQUID) was used to measure the magnetic properties of the $Ge_{1-x}Mn_x$ thin films and typical temperature-dependent hysteresis loops and magnetization moments in zero-field cooled (ZFC) and field cooled (FC) conditions (for sample S-5.5) are shown in Fig. 4(a and b), respectively. From Fig. 4(a), magnetic hysteresis loops is observable up to 300 K. This indicates a Curie temperature (T_c) of 300 K, which is confirmed by the FC-ZFC results (Fig. 4(b)). The result is similar to our

previous observation in the GeMn thin films grown on Si. Indeed, as mentioned above, Mn-rich clusters and precipitates (such as Mn_5Ge_3) exist in all examined samples. As a consequence, their magnetic properties are similar and mainly originated from the Mn-rich clusters and precipitates, as shown in Fig. 4. Particularly, from the FC-ZFC curves, a magnetic transition at around T_b = 26 K can be clearly observed in Fig. 4(b). As reported previously in the literature [16,24], this transition can be attributed to the blocking of coherent Mn-rich clusters (tadpoles or nanocolumns). As for another transition at T_b = 275 K, we attribute it to the formation of Mn_5Ge_3 precipitates, which also agrees with the previous results [16,24]. Note that the nanocolumn samples exhibit magnetic anisotropy when the external magnetic field direction changes from in-plane to out-of-plane. Consistent with our previous study [26], the easy axis typically lies in the out-of-plane direction because individual nanocolumn has a large shape anisotropy with greater dimension in the out-of-plane than that in the in-plane direction. However, in both directions, our study shows that the Curie temperature remains ~300 K with two blocking temperatures that are in the similar range. Finally, it is well documented that the room temperature T_c is originated from the Mn_5Ge_3 precipitates [16,24]. Overall, the magnetic properties of the GeMn thin films show the features of Mn-rich clusters and precipitates.

4. Conclusions

In conclusion, we have systematically examined the structural variations and magnetic properties of Mn-doped Ge thin films grown on Ge substrates by TEM, HRTEM and EDS. We demonstrated that the morphology of coherent Mn-rich clusters can be controlled from tadpole to nanocolumn by altering the nominal Mn concentration. For a 3.5% Mn-doped $Ge_{1-x}Mn_x$ thin film grown at 70 °C, a critical thickness of ~12 nm has been identified to form Mn-rich clusters. As Mn-rich clusters and precipitates exist in all samples, the GeMn thin films show a complex magnetic behaviors, which are mainly originated from the clusters and precipitates. Our results also reveal that a flat buffer layer surface plays a vital role to obtain vertically aligned tadpoles and nanocolumns.

References

[1] H. Ohno, Science 281 (1998) 951–956.
[2] T. Dietl, Semicond. Sci. Technol. 17 (2002) 377–392.
[3] Y. Wang, J. Zou, Y.J. Li, B. Zhang, W. Lu, Acta Mater. 57 (2009) 2291–2299.
[4] M.C. Bennett, M.C. Aronson, D.A. Sokolov, C. Henderson, Z. Fisk, J. Alloys Compd. 400 (2005) 2–10.
[5] Y.D. Park, A.T. Hanbicki, S.C. Erwin, C.S. Hellberg, J.M. Sullivan, J.E. Mattson, T.F. Ambrose, A. Wilson, G. Spanos, B.T. Jonker, Science 295 (2002) 651–654.
[6] F.X. Xiu, Y. Wang, J. Kim, A. Hong, J.S. Tang, A.P. Jacob, J. Zou, K.L. Wang, Nat. Mater. 9 (2010) 337–344.
[7] W.G. Zhu, H.H. Weitering, E.G. Wang, E. Kaxiras, Z.Y. Zhang, Phys. Rev. Lett. 93 (2004) 126102.
[8] A. Stroppa, S. Picozzi, A. Continenza, A.J. Freeman, Phys. Rev. B 68 (2003) 155203.
[9] J.S. Kang, G. Kim, S.C. Wi, S.S. Lee, S. Choi, S. Cho, S.W. Han, K.H. Kim, H.J. Song, H.J. Shin, A. Sekiyama, S. Kasai, S. Suga, B.I. Min, Phys. Rev. Lett. 94 (2005) 147202.
[10] J.X. Deng, Y.F. Tian, S.M. He, H.L. Bai, T.S. Xu, S.S. Yan, Y.Y. Dai, Y.X. Chen, G.L. Liu, L.M. Mei, Appl. Phys. Lett. 95 (2009) 062513.
[11] Y. Wang, J. Zou, Z.M. Zhao, X.H. Han, X.Y. Zhou, K.L. Wang, J. Appl. Phys. 103 (2008) 066104.
[12] S.Q. Zhou, D. Burger, A. Mucklich, C. Baumgart, W. Skorupa, C. Timm, P. Oesterlin, M. Helm, H. Schmidt, Phys. Rev. B 81 (2010) 165204.
[13] T. Devillers, M. Jamet, A. Barski, V. Poydenot, P. Bayle-Guillemaud, E. Bellet-Amalric, S. Cherifi, J. Cibert, Phys. Rev. B 76 (2007) 205306.
[14] C. Jaeger, C. Bihler, T. Vallaitis, S.T.B. Goennenwein, M. Opel, R. Gross, M.S. Brandt, Phys. Rev. B 74 (2006) 045330.
[15] J.P. Ayoub, L. Favre, I. Berbezier, A. Ronda, L. Morresi, N. Pinto, Appl. Phys. Lett. 91 (2007) 141920.
[16] S. Ahlers, D. Bougeard, N. Sircar, G. Abstreiter, A. Trampert, M. Opel, R. Gross, Phys. Rev. B 74 (2006) 214411.
[17] L. Ottaviano, M. Passacantando, S. Picozzi, A. Continenza, R. Gunnella, A. Verna, G. Bihlmayer, G. Impellizzeri, F. Priolo, Appl. Phys. Lett. 88 (2006) 061907.
[18] M. Passacantando, L. Ottaviano, F. D'Orazio, F. Lucari, M. De Biase, G. Impellizzeri, F. Priolo, Phys. Rev. B 73 (2006) 195207.
[19] C. Bihler, C. Jaeger, T. Vallaitis, M. Gjukic, M.S. Brandt, E. Pippel, J. Woltersdorf, U. Gosele, Appl. Phys. Lett. 88 (2006) 112506.
[20] T. Matsui, T. Fukushima, M. Shigematsu, H. Mabuchi, K. Morii, J. Alloys Compd. 236 (1996) 111–116.
[21] Y. Wang, J. Zou, Z.M. Zhao, X.H. Han, X.Y. Zhou, K.L. Wang, Appl. Phys. Lett. 92 (2008) 101903.
[22] E. Biegger, L. Staheli, M. Fonin, U. Rudiger, Y.S. Dedkov, J. Appl. Phys. 101 (2007) 103912.
[23] H.L. Li, Y.H. Wu, Z.B. Guo, P. Luo, S.J. Wang, J. Appl. Phys. 100 (2006) 103908.
[24] Y. Wang, F.X. Xiu, J. Zou, K.L. Wang, A.P. Jacob, Appl. Phys. Lett. 96 (2010) 051905.
[25] A.P. Li, C. Zeng, K. van Benthem, M.F. Chisholm, J. Shen, S. Rao, S.K. Dixit, L.C. Feldman, A.G. Petukhov, M. Foygel, H.H. Weitering, Phys. Rev. B 75 (2007) 201201.
[26] F.X. Xiu, Y. Wang, K. Wong, Y. Zhou, X.F. Kou, J. Zou, K.L. Wang, Nanotechnology 21 (2010) 255602.
[27] D. Bougeard, S. Ahlers, A. Trampert, N. Sircar, G. Abstreiter, Phys. Rev. Lett. 97 (2006) 237202.